Multiphoton Effects Enhanced due to Ultrafast Photon-Number Fluctuations

Kirill Yu. Spasibko,[1,2,*] Denis A. Kopylov,[3] Victor L. Krutyanskiy,[3,4] Tatiana V. Murzina,[3] Gerd Leuchs,[1,2] and Maria V. Chekhova[1,2,3]

[1]Max Planck Institute for the Science of Light, Staudtstraße 2, 91058 Erlangen, Germany
[2]University of Erlangen-Nürnberg, Staudtstraße 7/B2, 91058 Erlangen, Germany
[3]Department of Physics, M. V. Lomonosov Moscow State University, Leninskie Gory, 119991 Moscow, Russia
[4]Institute for Quantum Optics and Quantum Information ÖAW, Technikerstraße 21a, 6020 Innsbruck, Austria

(Received 12 September 2017; published 29 November 2017)

The rate of an n-photon effect generally scales as the nth order autocorrelation function of the incident light, which is high for light with strong photon-number fluctuations. Therefore, "noisy" light sources are much more efficient for multiphoton effects than coherent sources with the same mean power, pulse duration, and repetition rate. Here we generate optical harmonics of the order of 2–4 from a bright squeezed vacuum, a state of light consisting of only quantum noise with no coherent component. We observe up to 2 orders of magnitude enhancement in the generation of optical harmonics due to ultrafast photon-number fluctuations. This feature is especially important for the nonlinear optics of fragile structures, where the use of a noisy pump can considerably increase the effect without overcoming the damage threshold.

DOI: 10.1103/PhysRevLett.119.223603

Multiphoton processes are the essence of nonlinear optics. Optical harmonics generation [1] and multiphoton absorption [2], ionization [3], polymerization [4], or spectroscopy [5] are widely used in practical applications. In any multiphoton process, a certain number of photons of the initial radiation get annihilated to produce the effect. For this reason, the output signal of an n-photon process scales as the normally ordered nth order moment of the incident photon number, $\langle :N^n: \rangle \equiv \langle (a^\dagger)^n a^n \rangle$ [6,7], similar to the rate of n-photon coincidences [8] in a quantum optics experiment. It follows that the rate $R^{(n)}$ of an n-photon effect scales as the nth order normalized autocorrelation function of the incident light, $g^{(n)} \equiv \langle :N^n: \rangle / \langle N \rangle^n$ [6,7,9–18]:

$$R^{(n)} \sim g^{(n)} F^n, \tag{1}$$

where $F \sim \langle N \rangle$ is the input photon flux.

According to Eq. (1), the *statistical efficiency* of an n-photon effect [11–15], defined as

$$\xi^{(n)} \equiv \frac{R^{(n)}}{F^n}, \tag{2}$$

should scale with $g^{(n)}$.

Enhancement due to intensity fluctuations has been demonstrated for the second-harmonic generation [13,15] and, recently, also for two-photon absorption [18] from thermal light, for which $g^{(n)} = n!$. Instead of thermal light, one can use multimode laser light [11,12,14,17], as the latter has intensity fluctuations due to the contributions of different temporal modes. In fact, pulsed light is more efficient for n-photon processes than continuous-wave light with the same mean intensity for the same reason: It has a strong intensity modulation.

Nevertheless, usually one observes multiphoton effects with coherent light, for which $g^{(n)} = 1$. The reason is that thermal light with a high intensity is hard to produce; thermal radiation used in Refs. [15,18] was obtained from a below-threshold laser, which is not very bright. Another standard source of thermal light, a rotating ground glass disk, has not only low brightness but also very slow intensity fluctuations. As an efficient source, one would desire a bright pulsed one with each pulse having ultrafast intensity fluctuations.

Exceptionally interesting in this connection is the bright squeezed vacuum (BSV) [19–23] produced via high-gain parametric down-conversion (PDC). It can be extremely bright—up to hundreds of milliwatts mean power [24,25]—and has a highly fluctuating photon number. In fact, this state has no coherent component and consists of only quantum noise. Taken separately, the signal and idler BSV beams have thermal statistics; but whenever they are indistinguishable, the statistics show "superbunched" behavior with $g^{(n)} = (2n-1)!!$ [26–29]. This makes the BSV extremely efficient for multiphoton effects [16], as one can see from Fig. 1(a) showing $g^{(n)}(n)$ for coherent (black), thermal (red), and BSV (blue) light.

BSV intensity fluctuations are not only strong; they can be extremely fast as well. Because of the broad spectrum, whose bandwidth can reach 100–150 THz [34–36], a BSV generated through PDC can feature correlation times down to a few femtoseconds. For a pulsed broadband BSV, the intensity will fluctuate not only from pulse to pulse but also within a single pulse. Although pulse-to-pulse fluctuations could be, in principle, mimicked by modulating the beam, fluctuations within the pulse cannot.

The latter makes the BSV extremely valuable for nonlinear effects. Any nonlinear effect with an ultrashort

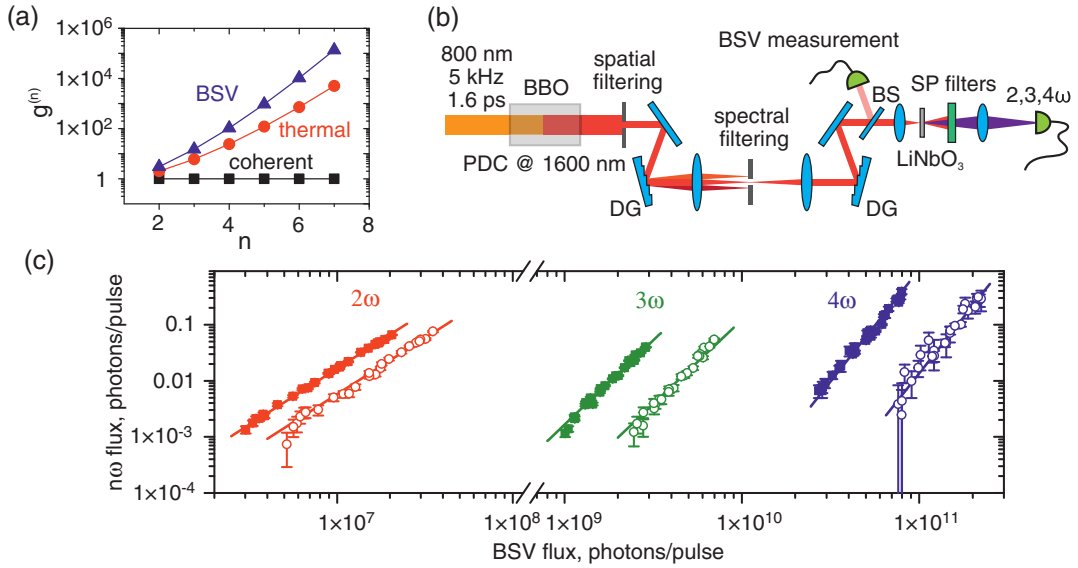

FIG. 1. (a) The normalized correlation function determining the enhancement of an n-photon effect as a function of n in the case of coherent (black), thermal (red), and BSV (blue) light used as a pump. (b) The experimental setup. The BSV is obtained via high-gain PDC in a BBO crystal and filtered spatially with a slit and spectrally with a $4f$ system containing two diffraction gratings (DG), two lenses, and a slit. After the filtering, a small part of the BSV is tapped off by a beam sampler (BS) for monitoring the mean photon number per pulse and the statistics, and the rest is tightly focused on the surface of a lithium niobate crystal ($LiNbO_3$). All optical harmonics are generated without phase matching, filtered from the BSV radiation with short-pass (SP) and bandpass filters and registered by a detector. (c) Measured dependence of the SHG (red), THG (green), and FHG (blue) photon flux on the pump flux with the pump being the BSV (solid squares) and pseudocoherent light (empty circles). The detection and transmission losses are taken into account [30]. Theoretical fits with the quadratic, cubic, and quartic functions (lines) show the correct power dependence for each harmonic.

response time will "feel" its fast photon-number fluctuations, and the efficiency will be therefore dramatically enhanced. In our experiment, we demonstrate this enhancement in the generation of the second (SHG), third (THG), and fourth (FHG) optical harmonics.

The experimental setup is shown in Fig. 1(b). For the generation of optical harmonics, we use a broadband BSV around the frequency degeneracy (1600 nm) [25] produced in a 10 mm beta barium borate (BBO) crystal through type-I phase matching. As a pump, we use the amplified radiation of a Ti-sapphire laser with the wavelength 800 nm, the pulse duration 1.6 ps, the repetition rate 5 kHz, and the energy per pulse 0.5 mJ. The pump is focused into the crystal by a cylindrical lens with a focal length of 700 mm, so that the beam remains unfocused in the plane of the optic axis and the pump walk-off [24] is not pronounced. After the crystal, we cut off the pump by dichroic mirrors and two long-pass filters. A slit is used to filter the BSV to a single spatial mode. The spectral filtering is made by a $4f$ monochromator. Although the bandwidth of the unfiltered BSV is 340 nm [25], the largest bandwidth allowed by filtering is 75 nm.

After spatial and spectral filtering, the BSV is tightly focused on the surface of a 1 mm thick lithium niobate crystal ($LiNbO_3$) slab by a lens with the focal length 3.1 mm and numerical aperture 0.68. For more efficient harmonic generation, the beam waist is placed on the crystal surface [37]. The crystal orientation does not allow phase matching for any harmonic generation. Both the BSV and all harmonics are polarized along the optic axis, which provides the highest nonlinear response in $LiNbO_3$. The radiation of optical harmonics is separated from the BSV by short-pass and bandpass filters. The photon number in each pulse of the harmonics radiation is measured with an avalanche photodiode (APD) or with a charge-integrating detector based on a Si p-i-n photodiode [22].

For monitoring and controlling the statistics of the BSV, we tap off 0.6% of its power and measure the numbers of photons in each pulse [30].

For each optical harmonic, we measure the dependence of the output photon flux $F_{n\omega}$ on the BSV flux F, spectrally filtered to a bandwidth of 3.3 nm. Figure 1(c) shows these dependences by red, green, and blue solid squares for the second, third, and fourth harmonics, respectively. The maximal harmonic generation efficiencies $\eta_{\max}^{(n)} \equiv F_{n\omega}/F$ are shown in Table I. The statistical efficiencies (2) can be obtained from the fits with the relevant dependencies, $f_n(x) = A^{(n)}x^n$, $n = 2, 3, 4$, shown by solid lines.

This has to be compared with the "standard" situation where the harmonics are generated from coherent light. In the absence of a coherent source with exactly the same wavelength, pulse duration, and repetition rate as the BSV, we create a pseudocoherent source by reducing the photon-number fluctuations of the BSV through postselection; i.e.,

TABLE I. Characteristics of the obtained harmonic generation from the BSV: statistical enhancement with respect to the pseudocoherent source ($A^{(n)}_{\mathrm{BSV}}/A^{(n)}_{\mathrm{pc}}$) (left), the ratios of the corresponding correlation functions $g^{(n)}_{\mathrm{BSV}}/g^{(n)}_{\mathrm{pc}}$ (center), and maximal harmonic generation efficiency $\eta^{(n)}_{\mathrm{max}}$ from Fig. 1(c) (right).

n	$A^{(n)}_{\mathrm{BSV}}/A^{(n)}_{\mathrm{pc}}$	$g^{(n)}_{\mathrm{BSV}}/g^{(n)}_{\mathrm{pc}}$	$\eta^{(n)}_{\mathrm{max}} \times 100\%$
2	2.86 ± 0.08	2.94 ± 0.06	$(3.2 \pm 0.3) \times 10^{-7}$
3	13.6 ± 0.8	14.5 ± 0.6	$(1.38 \pm 0.12) \times 10^{-9}$
4	71 ± 6	63 ± 2	$(4.9 \pm 0.7) \times 10^{-10}$

we register only pulses in which the number of photons in the BSV lies within certain boundaries. This way, we restrict the BSV fluctuations [38] and mimic the generation of optical harmonics from coherent light [30].

The power dependences for different harmonics generation from this pseudocoherent source are plotted in Fig. 1(c) by empty circles. One can see that the statistical efficiency is indeed considerably higher for the BSV than for pseudocoherent light. The enhancement factors are shown in Table I (second column), together with the ratios of the correlation functions for the BSV and the pseudocoherent light source (third column). As expected, there is an agreement between the two [39].

To compare the efficiency of harmonics generation from a degenerate BSV with the one from thermal light, we scan the BSV wavelength around the degeneracy point 1600 nm and measure the rates of the SHG, around 800 nm, of the THG, around 533 nm, and of the FHG, around 400 nm. The statistical efficiencies calculated according to Eq. (2) are plotted in Fig. 2, together with the corresponding correlation functions of the BSV. By scanning the wavelength, we pass from the BSV with thermal statistics (far from the degeneracy point) to the BSV with superbunched statistics (around the degeneracy point). The efficiency indeed follows the correlation function.

Next, we show that the efficiency of harmonic generation scales with the correlation functions also in the case of a broadband BSV. To control the statistics of the BSV in this case, we use an "unwanted" nonlinear process saturating the intensity fluctuations. Namely, BSV experiences further second-harmonic generation in the BBO crystal [30]. This process acts on the BSV as a nonlinear absorber. It reduces fluctuations by absorbing more photons from higher-energy bursts [40,41]. The contribution of this process can be tuned by tilting the crystal closer or further from the exact phase-matching position. With the crystal oriented far from the exact phase matching, the strong photon-number fluctuations of the BSV are maintained.

Figure 3 shows that the statistical efficiencies $\xi^{(n)}$ of SHG (left), THG (middle), and FHG (right) indeed follow the second-, third-, and fourth-order correlation functions of the BSV, respectively. Solid lines show linear fits $\xi^{(n)} \sim g^{(n)}$. In

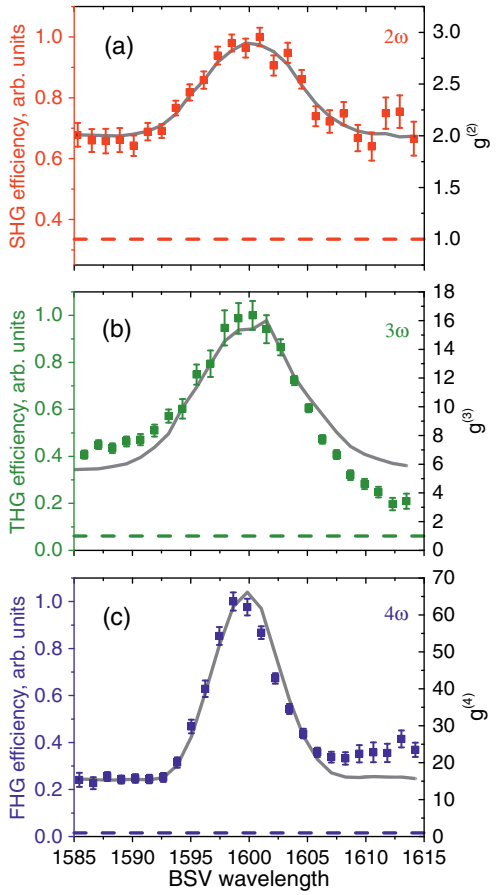

FIG. 2. SHG (a), THG (b), and FHG (c) statistical efficiencies $\xi^{(n)}$ (points) as well as the corresponding correlation functions (solid lines) measured versus the BSV wavelength. For comparison, the expected efficiencies for coherent light are shown by dashed lines.

all measurements, BSV is 75 nm broad, but, due to the slow response of the detectors, $g^{(n)}$ have to be measured under narrow-band (2.5 nm) filtering [30]. Otherwise, intensity fluctuations within each pulse lead to multimode detection and therefore to reduced values of correlation functions [42,43]. On the other hand, the generation of optical harmonics can be considered as a fast multiphoton detector [44,45], which "traces" fast fluctuations.

We see that the photon-number "noise" dramatically increases the efficiency of optical harmonic generation. It turns out that the generated harmonics are even "noisier" [9,15,46]. The correlation functions for the harmonics can be estimated from the ones for the pump. In particular, the second-order normalized correlation function $g^{(2)}_{n\omega}$ for the nth harmonics is [15,47]

$$g^{(2)}_{n\omega} = \frac{g^{(2n)}_{\omega}}{(g^{(n)}_{\omega})^2}. \tag{3}$$

Note that this formula is valid for any type of the pump statistics.

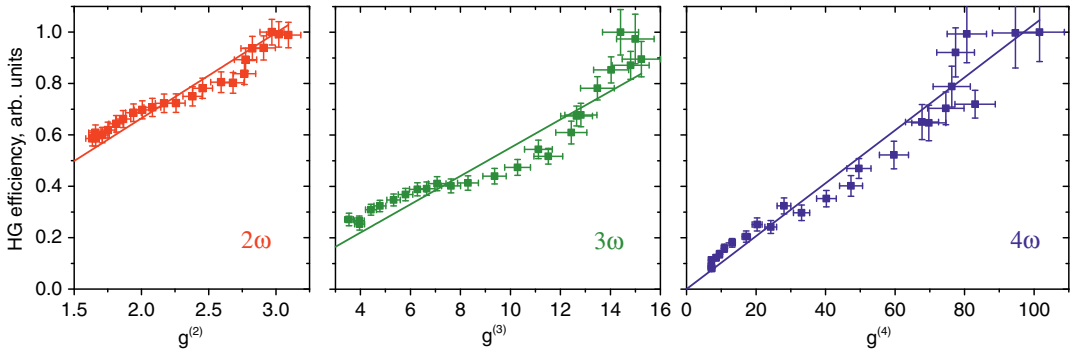

FIG. 3. Statistical efficiencies $\xi^{(n)}$ of SHG (left), THG (middle), and FHG (right) from a broadband BSV show linear dependences on the corresponding correlation functions, measured with narrow-band filtering. The correlation functions are varied by changing the orientation of the BBO crystal and hence the efficiency of BSV generation in the same crystal. Low values of the correlation functions are obtained with the BSV generated efficiently, so that the second-harmonic generation in BBO reduces the photon-number fluctuations. In the opposite case, with inefficient BSV generation, its superbunched statistics is almost perfectly preserved, and the correlation functions are high.

Figure 4 shows these values for all three optical harmonics generated from a superbunched (colored) and a thermal (shaded) BSV. The expected values are very high and range from 6, for SHG from thermal light [15,46], to 184, for FHG from a superbunched BSV. The experimental results, measured using a Hanbury Brown–Twiss setup with two APDs, are shown by circles on each bar. The data, in good agreement with the theory, show a huge increase of fluctuations in the generated optical harmonics.

These results, obtained for one particular case of optical harmonic generation, show that the BSV is an extremely useful source for multiphoton effects, in general. Among other applications, the use of a BSV as a pump will be beneficial for the multiphoton microscopy of fragile structures [48] including biological objects [49,50]. Indeed, in our experiment we generate harmonics without phase matching from extremely low mean powers (few nW to tens of μW). According to Fig. 1(c), a certain rate of a four-photon effect is achieved with a BSV having the mean power about 3 times less than in the case of coherent pumping. This can dramatically increase the sensitivity while not overcoming the damage threshold. It becomes most critical in the case of live cell imaging, where one should use the lowest possible photon dose [50].

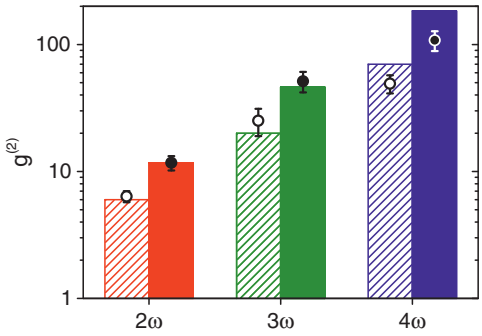

FIG. 4. Measured second-order autocorrelation functions $g^{(2)}_{n\omega}$ for the harmonics generated from a superbunched (solid circles) and a thermal (empty circles) BSV show extremely high fluctuations of the harmonic radiation, which increase with the number of the harmonic. The theoretical values are shown by solid and shaded color bars, respectively.

An important feature of the BSV is the time scale of its photon-number fluctuations. Here we have demonstrated a bandwidth of 9 THz, corresponding to times of 80 fs, but one can achieve times at least an order of magnitude shorter. Such behavior cannot be mimicked by any external intensity modulation. With such time scales, the BSV is useful for ultrafast spectroscopy, for example, for testing of materials response time. Although here for simplicity we used a single spatial mode, the multimode spatial structure of PDC will not change its noisy behavior, and one can use the whole frequency and angular spectrum of the BSV for exciting multiphoton effects.

Unlike a pulsed coherent source, the BSV has two typical times: the pulse duration and the intensity correlation time. Both parameters can be tuned in a broad range. This feature can be used in measurements considered in entangled-light spectroscopy [51,52] albeit with much larger photon fluxes than in the case of photon pairs.

Finally, the observation of extremely strong photon bunching in the radiation of optical harmonics from a BSV is very interesting in connection with the intensely discussed topic of extreme events and "rogue waves" [53], observed for processes with "heavy-tailed" probability distributions. The observed $g^{(2)} = 110 \pm 20$ is similar to the maximal values reported in the literature [54,55] and indicates a photon-number probability distribution with a very heavy tail. Because of the large dynamic range covered, such light can be used for the fast testing of the linear response of optical sensors. The perspective of observing multiphoton effects from such radiation is even more interesting; however, it would require a higher sensitivity than the one of our experiments.

We acknowledge the financial support of the joint DFG-RFBR (Deutsche Forschungsgemeinschaft - Russian Foundation for Basic Research) Project No. CH1591/2-1 - 16-52-12031 NNIOa and of the G-RISC (German-Russian Interdisciplinary Science Center) program, Projects No. P-2017a-19, No. P-2016a-5, and No. P-2016a-6.

*kirill.spasibko@mpl.mpg.de

[1] P. A. Franken, A. E. Hill, C. W. Peters, and G. Weinreich, Phys. Rev. Lett. **7**, 118 (1961).
[2] W. Denk, J. H. Strickler, and W. W. Webb, Science **248**, 73 (1990).
[3] N. B. Delone and V. P. Krainov, *Multiphoton Processes in Atoms* (Springer, Berlin, 2000).
[4] R. R. Gattass and E. Mazur, Nat. Photonics **2**, 219 (2008).
[5] Y. R. Shen, *The Principles of Nonlinear Optics* (Wiley, New York, 1984).
[6] B. R. Mollow, Phys. Rev. **175**, 1555 (1968).
[7] G. S. Agarwal, Phys. Rev. A **1**, 1445 (1970).
[8] R. J. Glauber, Phys. Rev. **130**, 2529 (1963).
[9] J. Ducuing and N. Bloembergen, Phys. Rev. **133**, A1493 (1964).
[10] P. Lambropoulos, C. Kikuchi, and R. K. Osborn, Phys. Rev. **144**, 1081 (1966).
[11] C. Lecompte, G. Mainfray, C. Manus, and F. Sanchez, Phys. Rev. A **11**, 1009 (1975).
[12] N. B. Delone and A. V. Masalov, Opt. Quantum Electron. **12**, 291 (1980).
[13] Y. Qu and S. Singh, Opt. Commun. **90**, 111 (1992).
[14] Y. Qu and S. Singh, Phys. Rev. A **47**, 3259 (1993).
[15] Y. Qu and S. Singh, Phys. Rev. A **51**, 2530 (1995).
[16] A. M. Popov and O. V. Tikhonova, J. Exp. Theor. Phys. **95**, 844 (2002).
[17] T. N. Smirnova and E. A. Tikhonov, Sov. J. Quantum Electron. **7**, 621 (1977).
[18] A. Jechow, M. Seefeldt, H. Kurzke, A. Heuer, and R. Menzel, Nat. Photonics **7**, 973 (2013).
[19] N. Corzo, A. M. Marino, K. M. Jones, and P. D. Lett, Opt. Express **19**, 21358 (2011).
[20] O. Jedrkiewicz, Y.-K. Jiang, E. Brambilla, A. Gatti, M. Bache, L. A. Lugiato, and P. Di Trapani, Phys. Rev. Lett. **93**, 243601 (2004).
[21] G. Brida, L. Caspani, A. Gatti, M. Genovese, A. Meda, and I. R. Berchera, Phys. Rev. Lett. **102**, 213602 (2009).
[22] T. Sh. Iskhakov, M. V. Chekhova, and G. Leuchs, Phys. Rev. Lett. **102**, 183602 (2009).
[23] I. N. Agafonov, M. V. Chekhova, and G. Leuchs, Phys. Rev. A **82**, 011801 (2010).
[24] A. M. Pérez, K. Yu. Spasibko, P. R. Sharapova, O. V. Tikhonova, G. Leuchs, and M. V. Chekhova, Nat. Commun. **6**, 7707 (2015).
[25] K. Yu. Spasibko, D. A. Kopylov, T. V. Murzina, G. Leuchs, and M. V. Chekhova, Opt. Lett. **41**, 2827 (2016).
[26] J. Janszky and Y. Yushin, Phys. Rev. A **36**, 1288 (1987).
[27] D. N. Klyshko, Phys. Usp. **39**, 573 (1996).
[28] F. Boitier, A. Godard, N. Dubreuil, P. Delaye, C. Fabre, and E. Rosencher, Nat. Commun. **2**, 425 (2011).
[29] T. Sh. Iskhakov, A. M. Pérez, K. Yu. Spasibko, M. V. Chekhova, and G. Leuchs, Opt. Lett. **37**, 1919 (2012).
[30] See Supplemental Material at http://link.aps.org/supplemental/10.1103/PhysRevLett.119.223603 for further details, which includes Refs. [31-33].
[31] L. Mandel and E. Wolf, *Optical Coherence and Quantum Optics* (Cambridge University Press, Cambridge, England, 1995).
[32] D. N. Klyshko, *Physical Foundations of Quantum Electronics* (World Scientific, Singapore, 2011).
[33] D. N. Klyshko and A. V. Masalov, Phys. Usp. **38**, 1203 (1995).
[34] D. Strekalov, A. B. Matsko, A. A. Savchenkov, and L. Maleki, J. Mod. Opt. **52**, 2233 (2005).
[35] M. Tiihonen, V. Pasiskevicius, A. Fragemann, C. Canalias, and F. Laurell, Appl. Phys. B **85**, 73 (2006).
[36] K. G. Katamadze, N. A. Borshchevskaya, I. V. Dyakonov, A. V. Paterova, and S. P. Kulik, Phys. Rev. A **92**, 023812 (2015).
[37] V. V. Rostovtseva, S. M. Saltiel, A. P. Sukhorukov, and V. G. Tunkin, Sov. J. Quantum Electron. **10**, 616 (1980).
[38] T. Sh. Iskhakov, V. C. Usenko, R. Filip, M. V. Chekhova, and G. Leuchs, Phys. Rev. A **93**, 043849 (2016).
[39] The fourth harmonic is produced with a reduced value of $g^{(4)} = 69 \pm 2$.
[40] J. Krasinski and S. Dinev, Opt. Commun. **18**, 424 (1976).
[41] G. Leuchs, NATO ASI Ser., Ser. B **135**, 329 (1986).
[42] O. A. Ivanova, T. Sh. Iskhakov, A. N. Penin, and M. V. Chekhova, Quantum Electron. **36**, 951 (2006).
[43] A. Christ, K. Laiho, A. Eckstein, K. N. Cassemiro, and C. Silberhorn, New J. Phys. **13**, 033027 (2011).
[44] A. Pe'er, B. Dayan, A. A. Friesem, and Y. Silberberg, Phys. Rev. Lett. **94**, 073601 (2005).
[45] S. Sensarn, G. Y. Yin, and S. E. Harris, Phys. Rev. Lett. **104**, 253602 (2010).
[46] A. Allevi and M. Bondani, Opt. Lett. **40**, 3089 (2015).
[47] M. C. Teich and G. J. Wolga, Phys. Rev. Lett. **16**, 625 (1966).
[48] V. K. Valev, A. V. Silhanek, Y. Jeyaram, D. Denkova, B. De Clercq, V. Petkov, X. Zheng, V. Volskiy, W. Gillijns, G. A. E. Vandenbosch, O. A. Aktsipetrov, M. Ameloot, V. V. Moshchalkov, and T. Verbiest, Phys. Rev. Lett. **106**, 226803 (2011).
[49] F. Helmchen and W. Denk, Nat. Methods **2**, 932 (2005).
[50] R. Cole, Cell Adhes. Migr. **8**, 452 (2014).
[51] M. G. Raymer, A. H. Marcus, J. R. Widom, and D. L. P. Vitullo, J. Phys. Chem. B **117**, 15559 (2013).
[52] K. E. Dorfman, F. Schlawin, and S. Mukamel, Rev. Mod. Phys. **88**, 045008 (2016).
[53] J. M. Dudley, F. Dias, M. Erkintalo, and G. Genty, Nat. Photonics **8**, 755 (2014).
[54] S. Meuret, L. H. G. Tizei, T. Cazimajou, R. Bourrellier, H. C. Chang, F. Treussart, and M. Kociak, Phys. Rev. Lett. **114**, 197401 (2015).
[55] S. Meuret, T. Coenen, H. Zeijlemaker, M. Latzel, S. Christiansen, S. Conesa-Boj, and A. Polman, Phys. Rev. B **96**, 035308 (2017).